Control-Based Stabilization of DC Microgrid for More Electric Aircraft

YANG Jiajun[1], *BUTICCHI Giampaolo*[1], *GU Chunyang*[1*],
WHEELER Pat[2], *ZHANG He*[1], *GERADA Chris*[2]

1. Key Laboratory of More Electric Aircraft Technology of Zhejiang Province, University of Nottingham Ningbo China, Ningbo 315000, P. R. China;

2. Power Electronics, Machines and Control Group, University of Nottingham, Nottingham NG7 2RD, U.K.

(Received 20 June 2021; revised 10 July 2021; accepted 12 September 2021)

Abstract: Electrifying the on-board subsystems of aircraft becomes an inevitable process as being faced with the environmental pollution, along with the proposed concept called more electric aircraft (MEA). With the increasing number of on-board power electronic based devices, the distribution system of the aircraft can be regarded as an on-board microgrid. As it is known that the load power electronic converters can exhibit constant power load (CPL) characteristics and reduce the system stability, it is necessary to accurately predict and enhance the system stability in designing process. This paper firstly analyzes the stability of an on-board DC microgrid with the presence of CPL. Then, discusses the reasons behind instability and proposes a control strategy to enhance system stability. Finally, the simulation results are worked out to validate the analysis and the effect of the proposed control strategy.

Key words: DC microgrid; stability analysis; impedance model; constant power load; more electric aircraft; dual active bridge converter; permanent magnet synchronous generator

CLC number: V242 **Document code:** A **Article ID:** 1005-1120(2021)05-0737-10

0 Introduction

Regarding to the deterioration of environment, it was proposed for aircraft that the on-board hydraulic, pneumatic, and mechanical subsystems need to be replaced with electrical subsystems. With these replacements, the proportion of electrical power increases, so called more electric aircraft (MEA). Compared with conventional aircraft, the MEA takes advantages of lower environmental impact, lower weight, and lower maintenance cost[1-3]. The process of electrifying on-board subsystems has been started recently. For example in Boeing 787, the wing de-icing system, the environmental control system and the engine starting system are powered electrically rather than powered pneumatically[3]. In addition, the starter/generator system is improved from constant speed drive (CSD) system to variable speed constant frequency (VSCF) system[4]. To be more detailed, the integrated drive generator (IDG) is removed, which was used to produce constant speed based on the variable speed of the jet engine[5]. As a solution, the generator is directly coupled to the jet engine through a gearbox. Besides, it was also proposed that the on-board AC microgrid can be replaced with DC microgrid. Compared with AC microgrid, the DC microgrid takes advantages of lower power losses on components, fewer conversion stages and lower bus current[6]. Fig.1 shows a DC microgrid containing 540 V high voltage (HV) DC buses and 28 V low voltage (LV) DC buses as potential for MEA.

As shown in Fig.1, the power electronic converters become the key element to achieve the con-

*Corresponding author, E-mail address: chunyang. gu@nottingham.edu.cn.

How to cite this article: YANG Jiajun, BUTICCHI Giampaolo, GU Chunyang, et al. Control-based stabilization of DC microgrid for more electric aircraft[J]. Transactions of Nanjing University of Aeronautics and Astronautics, 2021, 38(5): 737-746.
http://dx.doi.org/10.16356/j.1005-1120.2021.05.003

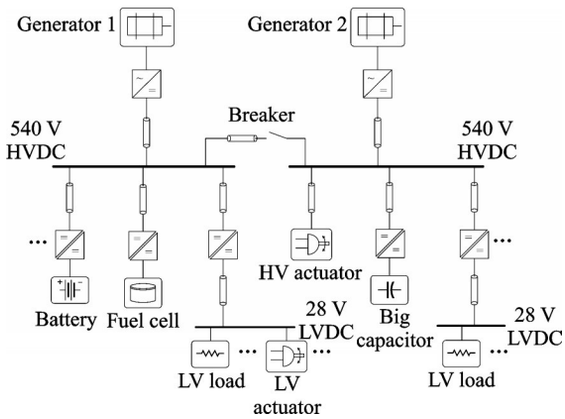

Fig.1 An example of DC microgrid for MEA

version between AC/DC voltage and different voltage levels, and there are varieties of loads interfaced with the converters, such as the loads insensitive to frequency, loads for energy storage, motors and pulsed loads. To be more detailed, the facilities for heating such as wing de-icing system, galley ovens and cargo heaters can be regarded as resistive loads, while the batteries, fuel cells and super capacitors are the loads for energy storage. Since these loads are tightly controlled by converters, the combination of the converters and the loads can be regarded as load subsystems, and the characteristics (such as power and impedance) of the load subsystems are determined by the characteristic of loads and the control strategy of converters. Unlike the resistive loads and energy storage units which have slow variation behavior during switching periods, the pulsed loads have fast and significant variation because they can instantly absorb large power from system, such as the radars and the electromagnetic launch and recovery systems. With this characteristic, the general averaging techniques such as switching averaging and state-space averaging cannot be applied directly. In this paper, the pulsed loads are not considered so that the later analysis is only valid if the amount of pulsed loads is a very minor part of the overall power requirements. As for the loads which have slow variations and require to be supplied with constant power, the subsystems to which the loads belong can be regarded as constant power load (CPL). CPL has characteristic of negative incremental impedance at operating point[7]. The I-V curve of CPL is shown in Fig.2.

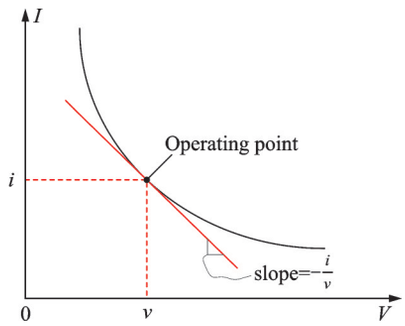

Fig.2 I-V curve of CPL

With such a behavior, the system stability can be a main concern. Hence, it is necessary to predict the system stability during design. So far, several approaches were proposed by researchers to assess the stability during system design. One main approach is based on the impedance. To implement this, the system needs to be decomposed into a source subsystem and a load subsystem. Fig.3 shows an equivalent circuit of a DC system, where V_S is an ideal voltage source, $V_{S,OUT}$ the output voltage of source subsystem, $V_{L,IN}$ the input voltage of load subsystem, Z_S the source impedance and Z_L the load impedance. Hence, the load voltage can be defined as

$$V_L = V_S \frac{Z_L}{Z_S + Z_L} = V_S \frac{1}{G_{MLG} + 1} \tag{1}$$

where $G_{MLG} = \dfrac{Z_S}{Z_L}$. Here a concept called minor loop gain G_{MLG} is introduced, which is defined as the ratio of source impedance and load impedance. It is worth mentioning that if the system is supplied by a current source I_S, the G_{MLG} will be reciprocal[8]. The load current can be given as

$$I_L = I_S \frac{Y_L}{Y_S + Y_L} = I_S \frac{1}{G_{MLG} + 1} \tag{2}$$

where Y_S is the source admittance, Y_L the load admittance, and $G_{MLG} = \dfrac{Y_S}{Y_L}$. With the minor loop gain, several impedance-based stability criteria were developed. The most basic one is the Nyquist Criterion that provides the sufficient and necessary condition for system stability. It depicts that for a system of which the source subsystem and load subsystem are individually stable, the whole system will be stable if the Nyquist contour of G_{MLG} does not encircle $(-1, 0)$. Based on that, other criteria were pro-

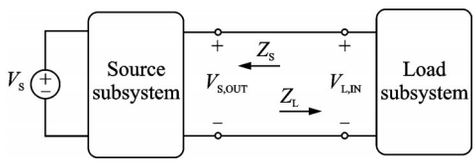

Fig.3 An equivalent circuit of a DC system

posed. The most conservative is Middlebrook Criterion since only the gain margin is considered[9]. The constraint is given as

$$\left|G_{MLG}\right| = \left|\frac{Z_S}{Z_L}\right| < \frac{1}{G_M} \qquad G_M > 1 \tag{3}$$

where G_M is the desired gain margin. Although the middlebrook criterion ensures the system stability, it sometimes results in overdesign since the size of input filter could be large. The gain margin phase margin (GMPM) criterion as a compromise mean, loose the requirement of system design by liberating the phase margin[10]. The constraint of GMPM criterion is given as

$$\begin{aligned} \left|G_{MLG}\right| &= \left|\frac{Z_S}{Z_L}\right| < \frac{1}{G_M} \\ \left|\angle G_{MLG}\right| &= \left|\angle Z_S - \angle Z_L\right| \leqslant 180° - P_M \end{aligned} \tag{4}$$

where G_M is the desired gain margin and P_M the desired phase margin. With such a constraint, the system can be optimized more while the system stability is guaranteed. Recently, there have been several research outcomes of the system stability analysis based on the impedance. The stability of a multi-source multi-load system with single DC bus is analyzed based on the impedance model[11]. The accurate impedance models of permanent magnet synchronous generator (PMSG) and dual active bridge (DAB) converter are validated and the relevant stability analysis is carried out[12], moreover, the individual stability of PMSG is analyzed based on its impedance model[13]. The instability of DC bus voltage of grid-connected voltage source converter (VSC) is analyzed based on the impedance model[14]. The stability of a three-phase AC system with CPL is analyzed in terms of d-q impedance[15]. In addition, the minor loop gain is modified when it comes to a single-bus system including converters with different types of control[16].

In this paper, the stability of a DC microgrid consisting of a PMSG as source, and a DAB converter and a permanent magnet synchronous motor (PMSM) as load, is analyzed in terms of their impedance models, where the impedance of bus cable is taken into consideration. Section 1 presents the impedance model of subsystems, and the system instability is pointed out by Bode diagram. Section 2 gives the explanations of system instability and proposes a method to mitigate the resonance resulted from the CLC circuit of DC system. Section 3 gives the simulation results of a switching model in PLECS. Section 4 draws the conclusion.

1 Impedance Model and System Instability

In this section, the output impedance of PMSG, input impedance of DAB converter and PMSM are given first, then the parameters of them and the DC bus cable are given. Next, the system instability is investigated.

1.1 Impedance model

The output impedance of PMSG has been derived[12-13] and given as

$$Z_{o,PMSG} = \frac{V_{dc}\left[G_i(s)+R_s+sL_s\right]}{sC_{PMSG}V_{dc}\left[G_i(s)+R_s+sL_s\right]+G_v(s)G_i(s)\left[1.5V_q-(R_s+sL_s)1.5I_q\right]G_{d,PMSG}(s)+I_o\left[G_i(s)+R_s+sL_s\right]G_{d,PMSG}(s)} \tag{5}$$

where V_{dc} is output DC voltage, C_{PMSG} the output capacitance, V_q the output voltage of q-axis current controller which will be transformed and applied to the rectifier, I_q the equivalent current on q-axis goes through the stator, I_o the output current of rectifier, $G_i(s)$ the transfer function of current controller and $G_v(s)$ the transfer function of DC link voltage controller, and $G_{d,PMSG}(s)$ the first-order delay function with time constant of one switching period. R_s and L_s are the stator resistance and inductance.

The input impedance of DAB converter has been derived[12,17] and given as

$$Z_{\mathrm{i,DAB}}=\frac{G_3G_{\mathrm{v,DAB}}R_{\mathrm{load}}+sC_{\mathrm{o}}R_{\mathrm{load}}+1}{G_4R_{\mathrm{load}}(G_2-G_1G_{\mathrm{v,DAB}})+sC_{\mathrm{i}}(G_3G_{\mathrm{v,DAB}}R_{\mathrm{load}}+sC_{\mathrm{o}}R_{\mathrm{load}}+1)} \tag{6}$$

where C_{i} is the input capacitance, C_{o} the output capacitance, R_{load} the load resistance, and $G_{\mathrm{v,DAB}}$ the transfer function of voltage controller. G_1, G_2, G_3 and G_4 are the small signal gains.

The control of PMSM is similar to the control of PMSG, except that the voltage controller is changed to be speed controller. In this case, the mechanical load torque is assumed to be constant. By considering that the bandwidth of current controller is large, it can quickly compensate the dynamics on DC link voltage by adjusting the output duty cycle. Hence, the PMSM is tightly controlled and the input impedance of PMSM can be given as

$$Z_{\mathrm{i,PMSM}}=-\frac{V_{\mathrm{i}}}{I_{\mathrm{i}}} \tag{7}$$

where V_{i} is the input DC voltage and I_{i} the input DC current.

1.2 Determination of DC bus cable parameters

According to the specifications of Airbus A380, the capacity of electrical power reaches 500 kW[3]. Since the DC bus voltage is chosen as 540 V, the rated current of bus cable must be larger than 1 000 A. Hence, the type of wire ASNE0438-YV AWG 4/0[18] is selected and seven of them are bundled up to be the cable to maximize the utilization of space. The cross-section is shown as Fig.4.

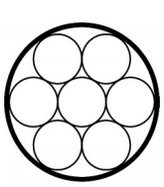

Fig.4 Cross-section of seven-wire bundled DC bus cable

Considering that the engines are located at the end of wings, it can be assumed that the length of bus cable is equal to the wingspan. With the known length and cross-section diameter of wire, the inductance of wire can be calculated using the formula[19], given as

$$L_{\mathrm{wire}}=2l\left\{\ln\left[\frac{2l}{d}\left(1+\sqrt{1+\left(\frac{d}{2l}\right)^2}\right)\right]-\sqrt{1+\left(\frac{d}{2l}\right)^2}+\frac{\mu}{4}+\frac{d}{2l}\right\} \tag{8}$$

where l is the length, d the cross-section diameter, and μ the relative permeability.

1.3 Specifications

Before analyzing the system stability, the parameters of PMSG, DAB converter and DC bus cable need to be given. To facilitate the process of selecting parameters, the parameters in Ref.[12] are used.

1.4 System instability

With the known impedance models and cable impedance, the system stability can be predicted using GMPM Criterion. As a criterion based on Bode diagram, GMPM Criterion requires proper grouping of subsystems since different groupings of subsystems can have different gain margin and phase margin for system design[20]. Hence, for converter-oriented design, the subsystems are regrouped and shown in Fig.5. With the known transfer functions of source impedance Z_{S} and load impedance Z_{L}, the Bode diagram of them at system power of 500 kW is obtained and shown in Fig.6. It can be seen that the Bode curves are intersected at frequency of about 570 Hz. At the frequency of intersection, the gain margin is minus and the phase margin is larger

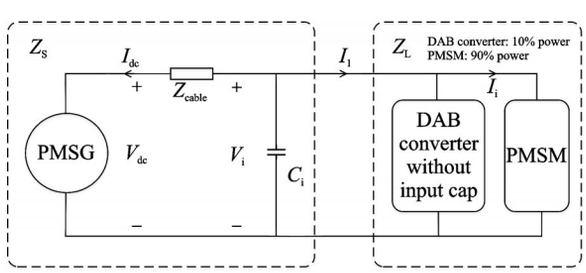

Fig.5 Grouping of subsystems

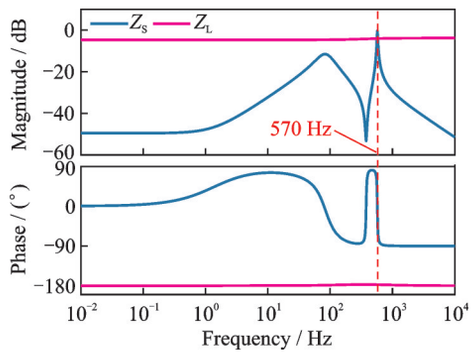

Fig.6 Bode diagrams of Z_S and Z_L at system power of 500 kW

than 180°. This means that the system will be unstable at system power of 500 kW, and the instability harmonics on DC bus has a main component with frequency of 570 Hz.

2 System Stabilization

2.1 System resonance

It is known that for a three-phase AC system, the widely used LCL filter could cause instability. However, for a DC system, the CLC circuit could be formed by the filter capacitance of converters and inductance of DC bus cable. In Fig.6, it also can be observed that the Bode curve of Z_S behaves as CLC circuit at high frequencies. The existence of CLC circuit in system can make resonance by charging and discharging process among filter capacitance and cable inductance, which can be a contribution to system instability. In this case, the output capacitance C_{PMSG} of PMSG, the inductance L_{wire} of DC bus cable and the input capacitor C_i of DAB converter form a CLC circuit (the resistance of bus cable is neglected here to simplify the computation process). The impedance of CLC circuit seen from the load side is given as

$$Z_{CLC}=\frac{C_{PMSG}L_{wire}s^2+1}{C_{PMSG}C_iL_{wire}s^3+(C_{PMSG}+C_i)s} \tag{9}$$

By re-arranging the terms in Eq.(8), it has

$$Z_{CLC}=\frac{1}{sC_i}\frac{s^2+\dfrac{1}{C_{PMSG}L_{wire}}}{s^2+\dfrac{C_{PMSG}+C_i}{C_{PMSG}C_iL_{wire}}} \tag{10}$$

Hence, the resonant frequency in radian of the CLC circuit can be obtained as

$$\omega_r=\sqrt{\frac{C_{PMSG}+C_i}{4\pi^2C_{PMSG}C_iL_{wire}}} \tag{11}$$

With the known values of C_{PMSG}, L_{wire} and C_i, the resonant frequency ω_r can be calculated. The calculated result shows a good match with the frequency labeled in Fig.6.

2.2 Proposed strategy for resonance mitigation

As discussed above, the resonance caused by the CLC circuit could make system tend to instability. If the resonance can be mitigated, the system stability can be enhanced. One main approach to suppress the resonance is proposing new control strategies. Considering that for PMSG the current control is directly applied to plant, and the bandwidth of inner current loop should be much larger than the outer voltage loop, the influence of current loop on performance of PMSG is dominated. Hence, to reshape the source impedance Z_S, the current control of PMSG is modified. Generally, the type of current control is proportional-integral (PI) control, which has good behavior of eliminating the DC error. The resonant control proposed in Ref.[21], which has good behavior of eliminating the AC error, is widely used in the stationary frame control of machine and grid. Taking account of the advantages of PI control and proportionnal resonant (PR) control, an ideal proportional-integral-resonant (PIR) control for DAB converter was proposed to eliminate the second-order harmonic component of the grid frequency waveforms in a DC grid in Ref.[22]. Here, the idea is to add resonant control into the current control. Hence, the type of current control becomes PIR control and can take care of both DC and AC errors. The transfer function of a non-ideal resonant controller is given as

$$G_r(s)=\frac{2k_r\omega_c s}{s^2+2\omega_c s+\omega_r^2} \tag{12}$$

where k_r is the resonant coefficient, ω_c the cut-off frequency in radian, and ω_r the desired resonant frequency in radian.

Before applying the controller, the selection of parameters becomes important. To investigate the impact of parameters on the performance of control-

ler, different parameters are set and the corresponding Bode curves are checked. Fig. 7 shows the Bode curves of PI controller and PIR controller with different parameters. Compared with PI controller, the PIR controller has the large gain at the resonant frequency. As for the PIR controller, increasing the cut-off frequency ω_c will slightly increase the gain and bandwidth of sideband centered on resonant frequency, while the gain at the resonant frequency keeps the same. In addition, increasing the resonant coefficient k_r will obviously increase the gain and the bandwidth of sideband centered on resonant frequency, and the gain at the resonant frequency is also increased. In this paper, the PI parameters of current controller are determined using pole-zero cancellation method[12-13]. As for the resonant controller, k_r is set as 1, ω_c is set as 50 Hz and ω_r is set as 570 Hz. Fig.8 shows the Bode diagram of open loop gain of current control loop using PI controller and PIR controller. It can be seen that the addition of resonant controller increases the gain at resonant frequency. Fig.9 shows the Bode diagram of Z_L and Z_S with PI and PIR current control of PMSG at system power of 500 kW. It can be seen that with PIR controller the gain of Z_S at 570 Hz is attenuated, avoiding the intersection with Z_L. Fig.10 shows the Nyquist contour of minor loop gain G_{MLG}. It can be seen that the contour with PI control encircles $(-1, 0)$, indicating that the system will be unstable, while the system becomes stable when PIR control is applied.

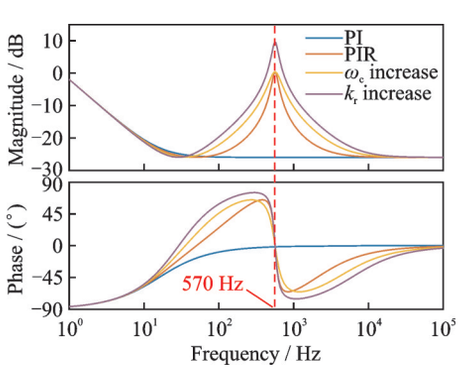

Fig.7 Bode diagrams of PI controller and PIR controller with different parameters

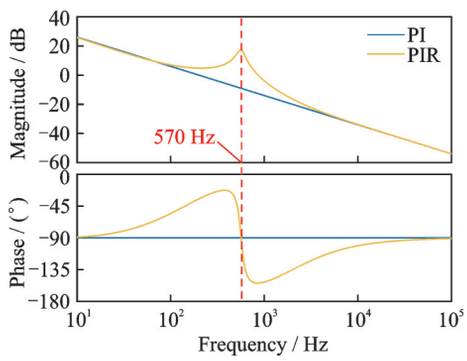

Fig.8 Bode diagrams of open loop gain of current control loop using PI controller and PIR controller

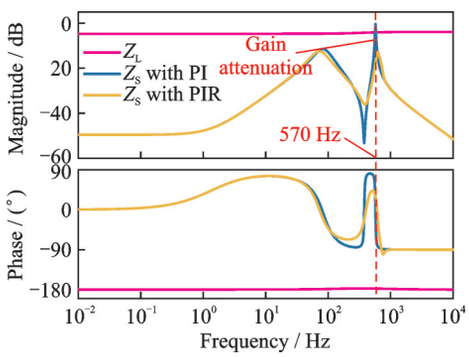

Fig.9 Bode diagrams of Z_L and Z_S with PI and PIR current control of PMSG at system power of 500 kW

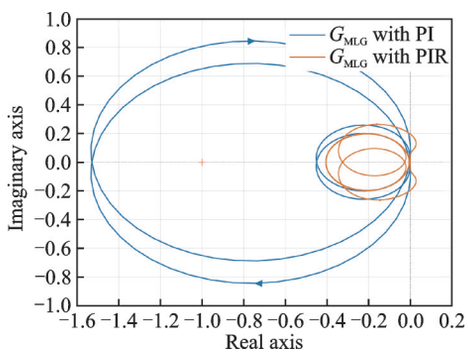

Fig.10 Nyquist contour of minor loop gain with PI and PIR control of PMSG at system power of 500 kW

3 Simulation Results

In this section, a switching model is built in PLECS to check the system instability caused by the resonance of CLC circuit and the effect of PIR controller on system stabilization. Fig.11 shows the simulation waveforms of output voltage and q-axis current of PMSG using PI current control. In Fig.11, the power of system is set as 300 kW initial-

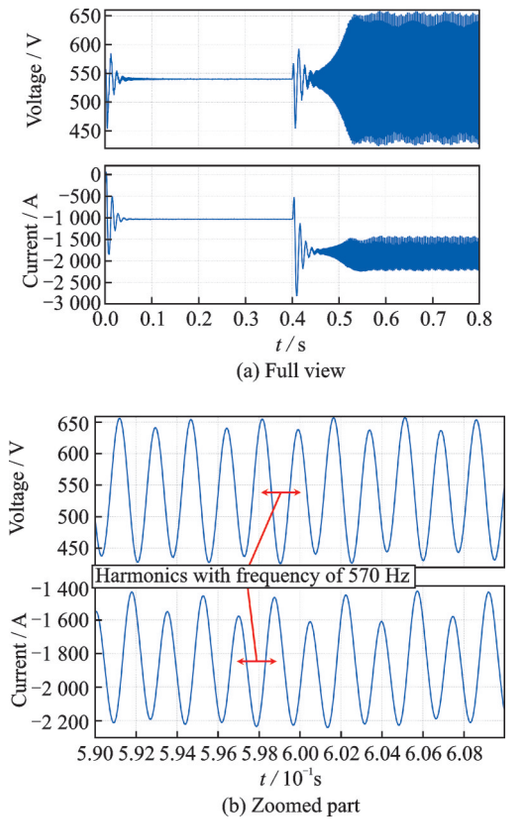

Fig.11 Simulation waveforms of output voltage and q-axis current of PMSG using PI control at $t = 0.6$ s

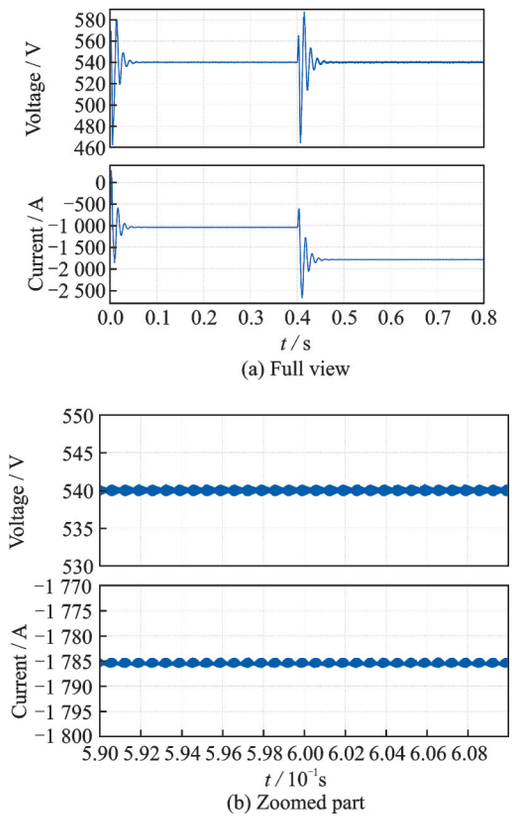

Fig.12 Simulation waveforms of output voltage and q-axis current of PMSG using PIR control at $t = 0.6$ s

ly and then increases to 500 kW at $t = 0.4$ s. It can be seen from Fig.11(a) that the system becomes unstable after t=0.4 s, and the frequency of instability harmonic component can be observed in Fig.11(b), which is 570 Hz. Hence, the simulation results are consistent with the prediction results of Bode diagram in Fig.6 and the Nyquist contour in Fig.10. Fig.12 shows the simulation waveforms of output voltage and q-axis current of PMSG using PIR controller. It can be seen from Fig.12(a) that with PIR controller the system keeps stable after the power stepped to 500 kW at $t = 0.4$ s. And it is shown in Fig.12(b) that the 570 Hz harmonic component is eliminated. These simulation results also show a good match with the prediction results of Bode diagram in Fig.9 and the Nyquist contour in Fig.10.

The simulation results presented above shows that the PIR current control has effect on suppressing the resonance of DC bus which is introduced by the capacitance and inductance on bus. With this feature, the stable region of system is extended, and the system power can go higher with the same parameters. In addition, the inductance of bus cable can be increased, and the input capacitance of load subsystems can be reduced meanwhile the size of capacitors is also optimized.

4 Conclusions

This paper analyzes the stability of an on-board DC microgrid based on the impedance models of subsystems. The system instability is pointed out from the Bode diagram, and the reasons behind it is revealed, that is, the instability is mainly due to the resonance of the CLC type circuit. To suppress the resonance, the resonant control is introduced into the current control of PMSG, to reshape the source impedance. It can be seen from the Bode diagram that the gain at the frequency of instability harmonic component is significantly attenuated. As for the validation, the simulation of a switching model is carried out. The simulation results are consistent with the predicted results by analysis.

References

[1] WHEELER P, BOZHKO S. The more electric aircraft: Technology and challenges[J]. IEEE Electrification Magazine, 2014, 2(4): 6-12.

[2] BUTICCHI G, BOZHKO S, LISERRE M, et al. On-board microgrids for the more electric aircraft—Technology review[J]. IEEE Transactions on Industrial Electronics, 2019,66(7): 5588-5599.

[3] MADONNA V, GIANGRANDE P, GALEA M. Electrical power generation in aircraft: Review, challenges, and opportunities[J]. IEEE Transactions on Transportation Electrification, 2018, 4(3): 646-659.

[4] EMADI K, EHSANI M. Aircraft power systems: Technology, state of the art, and future trends[J]. IEEE Aerospace and Electronic Systems Magazine, 2000,15(1): 28-32.

[5] SARLIOGLU B, MORRIS C T. More electric aircraft: Review, challenges, and opportunities for commercial transport aircraft[J]. IEEE Transactions on Transportation Electrification,2015,1(1): 54-64.

[6] SALOMONSSON D, SANNINO A. Low-voltage DC distribution system for commercial power systems with sensitive electronic loads[J]. IEEE Transactions on Power Delivery, 2007,22(3): 1620-1627.

[7] EMADI A, KHALIGH A, RIVETTA C H, et al. Constant power loads and negative impedance instability in automotive systems: Definition, modeling, stability, and control of power electronic converters and motor drives[J]. IEEE Transactions on Vehicular Technology, 2006, 55(4): 1112-1125.

[8] SUN J. Impedance-based stability criterion for grid-connected inverters[J]. IEEE Transactions on Power Electronics, 2011, 26(11): 3075-3078.

[9] MIDDLEBROOK R D. Input filter considerations in design and application of switching regulators[C]// Proceedings of PESC 76, IEEE Power Electronics Specialists Conference. [S.l.]: IEEE, 1976.

[10] WILDRICK C M, LEE F C, CHO B H, et al. A method of defining the load impedance specification for a stable distributed power system[J]. IEEE Transactions on Power Electronics, 1995,10(3): 280-285.

[11] GAO F, BOZHKO S. Modeling and impedance analysis of a single DC bus-based multiple-source multiple-load electrical power system[J]. IEEE Transactions on Transportation Electrification, 2016,2(3): 335-346.

[12] YANG J J, YAN H, GU C Y, et al. Modeling and stability enhancement of a permanent magnet synchronous generator based DC system for more electric aircraft[J]. IEEE Transactions on Industrial Electronics, 2021. DOI:10.1109/TIE.2021.3066934.

[13] YANG J J, BUTICCHI G, GU C Y, et al. Impedance-based stability analysis of permanent magnet synchronous generator for the more electric aircraft[C]// Proceedings of 2021 IEEE Workshop on Electrical Machines Design, Control and Diagnosis (WEMDCD). Modena, Italy: IEEE, 2021.

[14] LU Dapeng, WANG Xiongfei, BLAABJERG F, et al. Impedance-based analysis of DC-Link voltage dynamics in voltage-source converters[J]. IEEE Transactions on Power Electronics, 2019, 34(4): 3973-3985.

[15] WEN B, BOROYEVICH D, BURGOS R, et al. Small-signal stability analysis of three-phase AC systems in the presence of constant power loads based on measured *d-q* frame impedances[J]. IEEE Transactions on Power Electronics, 2015, 30(10): 5952-5963.

[16] ZHANG X, RUAN X, TSE C K. Impedance-based local stability criterion for DC distributed power systems[J]. IEEE Transactions on Circuits and Systems I: Regular papers, 2015, 62(3): 1-10.

[17] YANG J, BUTICCHI G, YAN H, et al. Impedance-based sensitivity analysis of dual active bridge DC-DC converter[C]//Proceedings of 2019 IEEE the 13th International Conference on Compatibility, Power Electronics and Power Engineering (CPE-POWERENG). [S.l.]:IEEE, 2019.

[18] Nexans. Aircraft wires and cables[M]. [S.l.]: Nexans, 2007.

[19] GROVER F W. Inductance calculations: Working formulas and tables[M]. New York: Instrument Society America, 1946.

[20] SUDHOFF S D, GLOVER S F, LAMM P T, et al. Admittance space stability analysis of power electronic systems[J]. IEEE Transactions on Aerospace and Electronic Systems, 2000,36(3): 965-973.

[21] ZMOOD D N, HOLMES D G. Stationary frame current regulation of PWM inverters with zero steady-state error[J]. IEEE Transactions on Power Electronics, 2003, 18(3): 814-822.

[22] QIN H, KIMBALL J W. Closed-loop control of DC-DC dual-active-bridge converters driving single-

phase inverters[J]. IEEE Transactions on Power Electronics, 2014, 29(2): 1006-1017.

Acknowledgements This work was supported by Ministry of Science & Technology under National Key R&D Program of China (No. 2021YFE0108600), Ningbo Science and Technology Bureau under S&T Innovation 2025 Major Special Program (No. 2019B10071), and the Key International Cooperation of National Natural Science Foundation of China (No.51920105011).

Authors Mr. **YANG Jiajun** received the B.E. degree (Hons.) in electrical and electronic engineering in 2017, from the University of Nottingham Ningbo China, Ningbo, China, where he is currently working toward the Ph.D. degree with the Key Laboratory of More Electric Aircraft Technology of Zhejiang Province. From 2017 to 2018, he was a hardware engineer with the Nottingham Electrification Centre. His current research interests include high power density DC-DC converters and stability analysis of DC microgrids for the more electric aircraft.

Prof. **BUTICCHI Giampaolo** received the Master degree in Electronic Engineering in 2009 and the Ph.D. degree in Information Technologies in 2013 from the University of Parma, Italy. In 2012 he was the visiting researcher at the University of Nottingham, UK. Between 2014 and 2017, he was a postdoctoral researcher, and Guest Professor at the University of Kiel, Germany. During his stay in Germany, he was awarded with the Von Humboldt Postdoctoral Fellowship to carry out research related to fault tolerant topologies of smart transformers. In 2017 he was appointed as associate professor in Electrical Engineering at the University of Nottingham Ningbo China and as head of Power Electronics of the Nottingham Electrification Center. He was promoted to Professor in 2020. His research focuses on power electronics for renewable energy systems, smart transformer fed micro-grids and DC grids for the more electric aircraft. Dr. BUTICCHI is one of the advocates for DC distribution systems and multiport power electronics onboard the future aircraft. He is author/co-author of more than 230 scientific papers, an associate editor of the IEEE Transactions on Industrial Electronics, the IEEE Transactions on Transportation Electrification and the IEEE Open Journal of the Industrial Electronics Society. He is currently the Chair of the IEEE-IES Technical Committee on Renewable Energy Systems and the IES Energy Cluster Delegate.

Dr. **GU Chunyang** received Ph.D. degree from Tsinghua University in electrical engineering, Beijing, China, in 2015. In 2015, she went to the University of Nottingham, UK, where she was a postdoc research fellow in Power Electronics, Machines and Control (PEMC) Research Group. Since 2017, she has been an assistant professor in Department of Electrical and Electronic Engineering and PEMC Research Group, University of Nottingham Ningbo China. Her research interests include power electronics for transportation electrification, renewable energy and grid applications, e.g. solid-state transformer, solid-state circuit breaker, multi-level converter topologies and control, application of wide-band-gap semiconductor devices, power electronics in EV, railway, marine and more electric aircraft.

Prof. **WHEELER Pat** received his BEng [Hons] degree in 1990 from the University of Bristol, UK. He received his Ph.D. degree in Electrical Engineering for his work on matrix converters from the University of Bristol, UK in 1994. In 1993 he moved to the University of Nottingham and worked as a research assistant in the Department of Electrical and Electronic Engineering. In 1996 he became a lecturer in the Power Electronics, Machines and Control Group at the University of Nottingham, UK. Since January 2008 he has been a full professor in the same research group. He was head of the Department of Electrical and Electronic Engineering at the University of Nottingham from 2015 to 2018. He is currently the head of the Power Electronics, Machines and Control Research Group, global director of the University of Nottingham as Institute of Aerosapce Technology and was the Li Dak Sum Chair Professor in Electrical and Aerospace Engineering. He is a member of the IEEE PELs AdCom and is currently an IEEE PELS Vice-President. He has published over 750 academic publications in leading international conferences and journals.

Prof. **ZHANG He** received his B.Eng degree in Control Science and Engineering from Zhejiang University, China, in 2002. He obtained the MSc and Ph. D. degree in electrical machines from The University of Nottingham, UK, in 2004 and 2009 respectively. After this he worked as research fellow at the University and director of BestMotion Technology Centre. He moved to University of Nottingham Ningbo China as senior research fellow in 2014, promoted to principal research fellow in 2016 and to professor in 2020. Currently he is the director of Nottingham Electrification Centre within the Power Electronics, Machines and Control Research Group in University of Nottingham. His research interests include high performance electric machines and drives for trans-

port electrification.

Prof. **GERADA Chris** received the Ph.D. degree in numerical modeling of electrical machines from the University of Nottingham, Nottingham, UK, in 2005. He subsequently worked as a researcher with the University of Nottingham on high performance electrical drives and on the design and modeling of electromagnetic actuators for aerospace applications. In 2008, he was appointed as a lecturer in Electrical Machines, in 2011, as an associate professor, and in 2013, as a professor with the University of Nottingham. His main research interests include the design and modeling of high-performance electric drives and machines. He serves as an associate editor for the IEEE Transactions on Industry Applications and is the past chairman of the IEEE IES Electrical Machines Committee.

Author contributions Mr. **YANG Jiajun** designed the study, derived the impedance models, conducted the stability analysis, interpreted the results and wrote the manuscript. Prof. **BUTICCHI Giampaolo**, Dr. **GU Chunyang** and Prof. **WHEELER Pat** contributed to the discussion and background of the study. Prof. **ZHANG He** and Prof. **GERADA Chris** provides the software and research platform for this study. All authors commented on the manuscript draft and approved the submission.

Competing interests The authors declare no competing interests.

(Production Editor: SUN Jing)

基于控制的多电飞机直流微电网稳定化

杨佳俊[1], BUTICCHI Giampaolo[1], 顾春阳[1],

WHEELER Pat[2], 张何[1], GERADA Chris[2]

(1. 宁波诺丁汉大学浙江省多电飞机重点实验室, 宁波 315000, 中国;
2. 英国诺丁汉大学电力电子、机器与控制研发组, 诺丁汉 NG7 2RD, 英国)

摘要: 面对日益严峻的环境污染, 飞机机载子系统的电气化过程已不可避免, 相应的多电飞机(More electric aircraft, MEA)的概念也因此被提出。随着机载电力电子设备数量的增加, 飞机上的配电系统可以被视作一个机载微电网。由于电力电子变换器工作时呈现恒功率负载(Constant power load, CPL)特性并降低系统稳定性, 在设计系统时需要精确预测并增强系统的稳定性。文中首先分析了包含CPL的机载直流微电网的稳定性, 然后探讨了不稳定现象背后的原因, 并提出了对应的控制策略来增强系统稳定性, 最后通过一系列的仿真结果来验证稳定性分析的准确性以及所提控制策略的效果。

关键词: 直流微电网; 稳定性分析; 阻抗模型; 恒功率负载; 多电飞机; 双有源桥变换器; 永磁同步发电机